

Hybrid semiconductor-atomic interface: slowing down single photons from a quantum dot

N. Akopian^{1*}, L. Wang², A. Rastelli², O. G. Schmidt² and V. Zwiller¹

Hybrid interfaces between semiconductor quantum dots and atomic systems could be of potential fundamental and technological interest, because they can combine the advantages of both constituents. Semiconductor quantum dots are tunable and deterministic sources of single¹ and entangled photons². Atomic vapours are widely used as slow-light media^{3,4} and quantum memories^{5,6}. Merging both systems could enable the storage of quantum dot emission—an important step towards the implementation of quantum memories and quantum repeaters⁷. Here, we show a hybrid semiconductor-atomic interface for slowing down single photons emitted from a single quantum dot. We use a double absorption resonance⁴ in rubidium vapour to create a slow-light medium in which a single photon is stored for 15 times its temporal width. Our result is the first demonstration of non-classical light storage, where single photons are generated on demand from a semiconductor source.

Slow light can be realized in atomic vapours by creating a medium with low group velocity^{3,4}. Early works, based on electromagnetically induced transparency⁸ (EIT), have already demonstrated group velocities of a few metres per second³. In later works, low group velocities were reported for single-photon pulses generated from atomic ensembles^{9,10}. Recently, slow light has also been demonstrated in hollow-core fibres^{11,12} and in on-chip hollow-core waveguides¹³. In EIT-based techniques, however, a spectrally narrow and temporally wide propagating pulse is usually used, and quantum dot generated photons are spectrally broader by two orders of magnitude. A double absorption resonance technique has been proposed to overcome these problems and has been used to slow down classical light⁴. In the present work, we take advantage of this approach and apply it to quantum dots that we have specially designed for our experiments¹⁴.

We first outline the relevant characteristics of the two systems that we couple: a single GaAs quantum dot (also known as an artificial atom¹⁵) and natural atoms (rubidium). Energy level diagrams and the relevant optical transitions in the quantum dot and rubidium are presented in Fig. 1a. Our GaAs quantum dots were designed to generate photons around 780 nm, close to the ⁸⁷Rb D_2 transitions¹⁴. The radiative recombination of a single electron-hole pair, an exciton, generates a single photon with wavelength, polarization and linewidth set by the quantum dot selection rules¹⁶. In particular, charge fluctuations in the vicinity of the quantum dot cause spectral diffusion of the emission, resulting in inhomogeneous broadening of the exciton line. Unlike other sources such as weak laser pulses or parametric down-conversion, which produce photons randomly, a quantum dot is a deterministic source of single photons¹. The quantum dot emission wavelength can be fine-tuned to rubidium transitions with external magnetic or electric fields¹⁴. In our interface we use the D_2 transitions in ⁸⁷Rb at the characteristic wavelength of 780 nm. The ground state

has a hyperfine splitting composed of two absorption resonances separated by $\sim 28 \mu\text{eV}$.

The photons emitted from a single quantum dot propagate through the rubidium vapour, are dispersed by a monochromator, and are detected by a charge-coupled device or single-photon detector for spectroscopy or temporal measurements. Photons emitted from a quantum dot can be tuned to match exactly the atomic transitions or to fall between the two lines of the hyperfine structure of the ground state. A schematic of the experiment is presented in Fig. 1b, and the coupling between artificial and natural atoms is demonstrated by the experimental data presented in Fig. 1c. We tune the emission of a quantum dot exciton through the D_2 transitions of ⁸⁷Rb by applying an external magnetic field to the quantum dot. The quantum dot exciton undergoes a Zeeman splitting and a diamagnetic shift with increasing magnetic field. As a result, each of the two branches can be controllably tuned to the D_2 transition of ⁸⁷Rb, and is partially absorbed by the vapour when in resonance.

For our slow-light experiments we tune the emission of a quantum dot within the hyperfine structure of the D_2 transitions and detect the arrival time of the emitted photons for various temperatures of the vapour cell. The ground state of the D_2 transitions consists of two Lorentzian absorption resonances. When the spacing between the resonances is small, $28 \mu\text{eV}$ for the D_2 transitions, a dispersion region is created, resulting in a steep refractive-index slope that depends on the atomic density⁴. The speed of photons with frequency between the D_2 transitions will be reduced, as we quantitatively demonstrate in our model below. As a result, these photons will be delayed and detected at later times than the photons with frequency outside the D_2 transitions. In the rubidium cell, the slow-light electromagnetic mode has the same peak intensity and power density but is compressed in size¹⁷, as illustrated in the inset of Fig. 2a. The experimental results are presented in Fig. 2a, which shows the histograms of detection events for various vapour temperatures. In this experiment the exciton emission of the quantum dot is tuned into resonance with the D_2 transitions of ⁸⁷Rb using a magnetic field of 7.8 T, and is spectrally filtered from the rest of the quantum dot emission for temporal measurements. As is clearly shown in the figure, part of the emitted photons is delayed and is partially absorbed by the vapour. Both delay and absorption increase with vapour temperature.

To describe the experimental result in Fig. 2a, we developed a theoretical model that accurately demonstrates the time evolution of photons composing the emission line of a quantum dot, while taking into account realistic experimental parameters. The results of the model for our experimental case are shown in Fig. 3a. The delay and absorption are strongly dependent on emission frequency. Outside the rubidium resonances, the delay and absorption are small, less than 1 ns and several percent, respectively. The delay

¹Kavli Institute of Nanoscience Delft, Delft University of Technology, 2628CJ Delft, The Netherlands, ²Institute for Integrative Nanosciences, IFW Dresden, 01069 Dresden, Germany. *e-mail: n.akopian@tudelft.nl

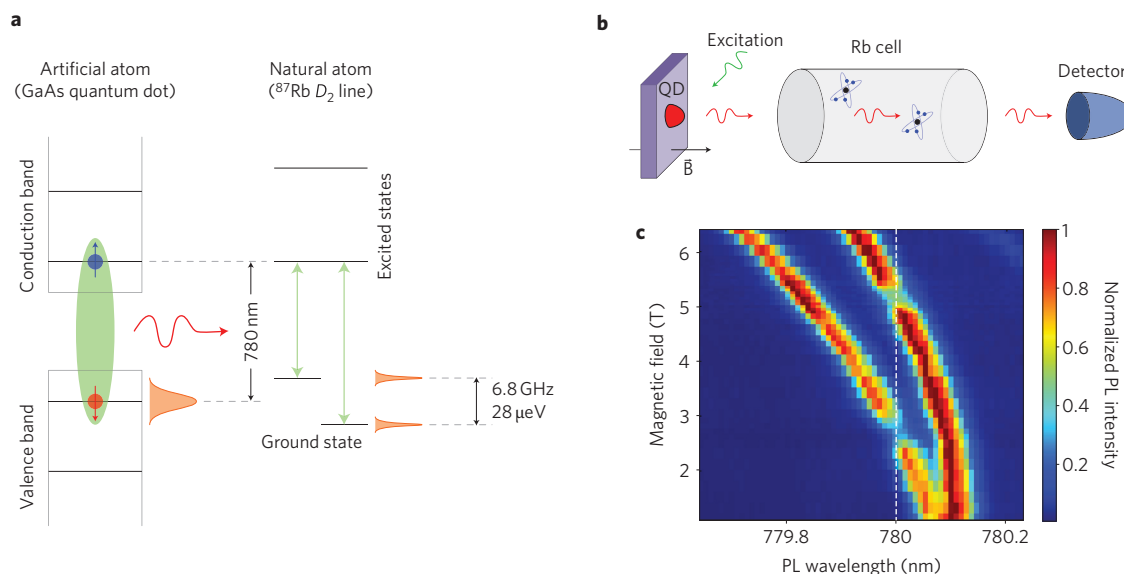


Figure 1 | Coupling natural and artificial atoms. **a**, Energy level diagrams in quantum dot and rubidium. The blue circle represents an electron, the red circle a hole, and the arrows their spin projections. The hyperfine structure of the ^{87}Rb D_2 ground state is $28 \mu\text{eV}$. Relevant, Fourier-limited optical transitions in quantum dots and rubidium are shown in green and are represented by orange Lorentzians. **b**, Schematics of the experiment. An optically excited quantum dot (QD) emits single photons, which propagate through the cell with a warm rubidium vapour before detection. **c**, Photoluminescence (PL) spectra of a quantum dot exciton under increasing magnetic field. The quantum dot was excited with a 532 nm continuous-wave laser. A cell with a rubidium vapour at 120°C was placed in front of the detector. Dashed line corresponds to the ^{87}Rb D_2 transitions and is partially absorbed by the vapour.

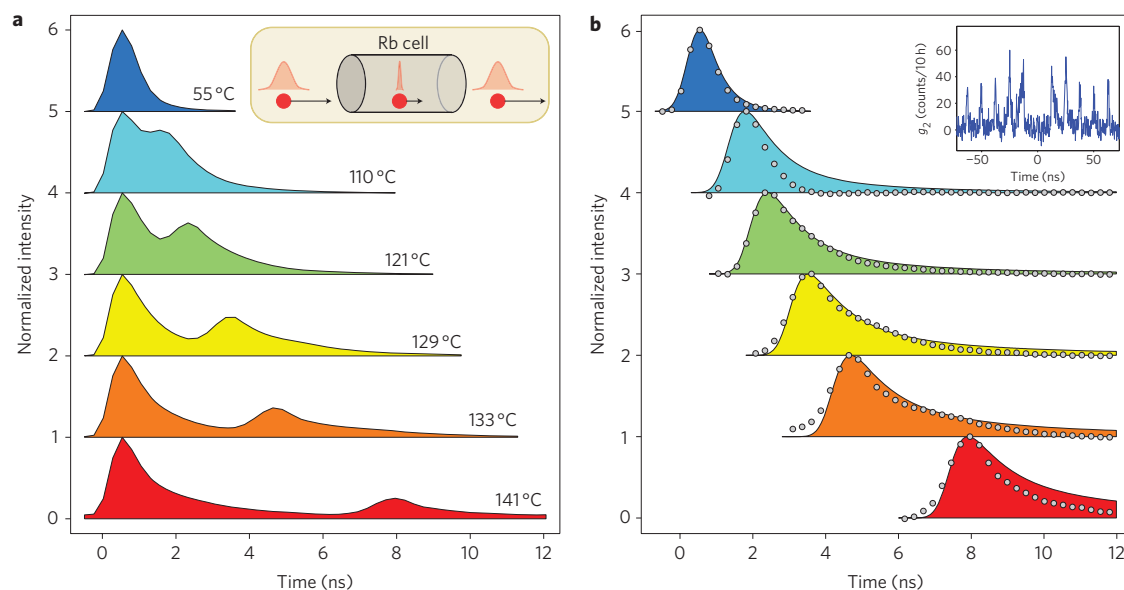


Figure 2 | Experimental demonstration of slow single photons from a quantum dot. **a**, Histograms of detection times of single photons with a rubidium vapour cell on the path. The quantum dot was excited with a 745 nm picosecond pulsed laser. Temperature of the cell: 55, 110, 121, 129, 133 and 141°C . Photons are slowed down in the rubidium cell and are detected at later times with increased vapour temperature, as demonstrated by the delayed peak. Inset: slow light in a rubidium cell. Photons are represented by red circles, velocities by arrows and their spatial distributions by solid curves. As a photon enters the cell containing rubidium vapour, its velocity is reduced and its electromagnetic mode is spatially compressed. The peak intensity and power density of the photon, however, remain unchanged. **b**, Filtered experimental data (circles), representing only photons slowed down in the cell (see Supplementary Information), together with the calculated delay (solid line). Photons propagating through the rubidium cell at 141°C are delayed by 7.5 ns with respect to the photons travelling through the cell at 55°C . Inset: temporal autocorrelation histogram of quantum dot exciton emission under pulsed laser excitation. The missing correlation events at time 0 demonstrate that the emission originates from a single-photon source.

becomes extremely long for photons with frequencies very close to the rubidium resonances. However, the extremely strong absorption there prevents them from being detected. The optimal frequency range lies between the two resonances, where the photons are

significantly delayed (~ 8 ns for a temperature of 141°C), and the absorption is weak ($\sim 25\%$). The blue curve on the right represents the evolution of the whole emission. It reproduces the experimental result (the measurement at 141°C shown in Fig. 2a). If the quantum

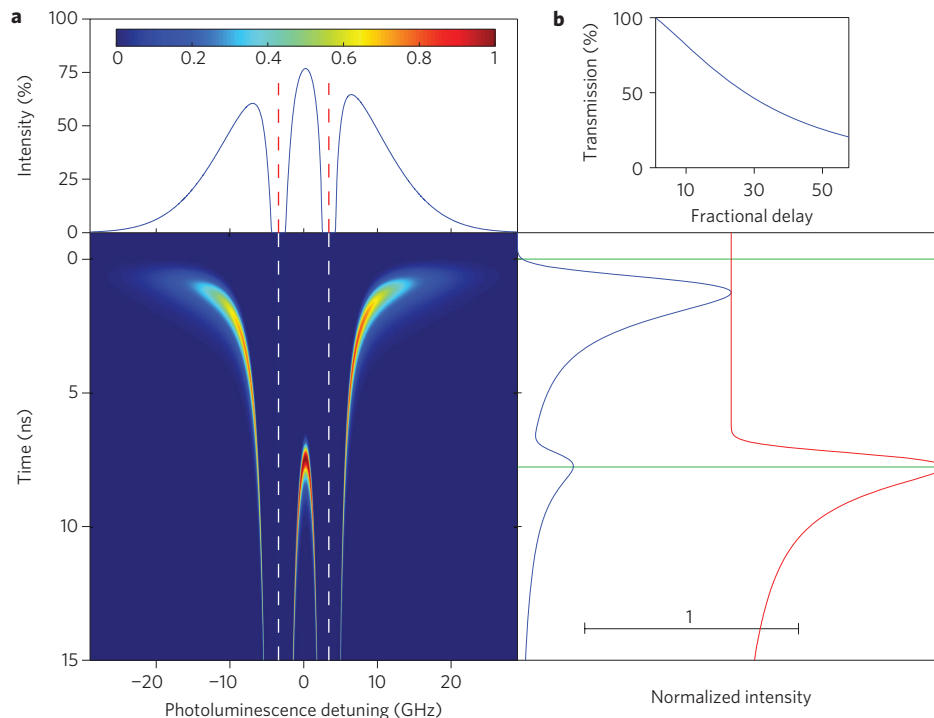


Figure 3 | Modelling and analysis of photon delay. **a**, False-colour plot showing the evolution of photons transmitted through a rubidium cell as a function of their detuning from the middle of the ground-state hyperfine structure of the ^{87}Rb D_2 transitions. Intensity is encoded in the colour bar. The total transmitted photoluminescence intensity is shown on top. The blue curve on the right represents evolution of the whole photoluminescence. The red curve corresponds to spectrally filtered photons with a frequency between the D_2 transitions, indicated by dashed lines. Green lines indicate zero and maximal peak delay. Maximum values in each plot are normalized to unity. Calculations were performed for the following experimental parameter set: rubidium vapour temperature, 141 °C; quantum dot emission lifetime and linewidth, 500 ps and 80 μeV , respectively. **b**, Transmission of the rubidium cell as a function of fractional delay for photons, which are only homogeneously broadened, with a lifetime of 500 ps and a corresponding Fourier-limited linewidth of 1.3 μeV (315 MHz).

dot emission linewidth is narrower than the hyperfine structure, all of the transmitted photons will be delayed, and the broader emission can be spectrally filtered, as shown by the red curve in Fig. 3a. The maximal peak delay remains the same for both blue and red curves, implying that photons from a spectrally isolated quantum dot with a Fourier-limited linewidth will have the same maximal delay as photons from a quantum dot that suffers from spectral diffusion.

The figure of merit of such delay systems is, however, not the absolute delay, but the fractional delay, defined as the ratio between the absolute delay and the temporal width of the propagating pulse. For an exponentially decaying quantum dot exciton emission we use its lifetime as a pulse temporal width. In Fig. 3b we show the calculated transmission of the rubidium cell as function of fractional delay for homogeneously broadened photons with Fourier-limited linewidth. The data show that photons can be significantly delayed with relatively small losses: for instance, up to 27 times their temporal width with losses lower than 50%.

In Fig. 2b we consider photons with frequencies between the two hyperfine split lines. This is done by subtracting from each measurement in Fig. 2a a fit that corresponds to the non-delayed photons that are spectrally outside the double resonance and are thus not delayed (see Supplementary Information). The experimental data are presented together with the model (the red curve in Fig. 3a) with only one parameter to fit, the temperature-dependent atomic density. The other parameters are fixed and their values are taken directly from the experimental data: the spectral linewidth and the lifetime of the emitted photons, the vapour temperature and the temporal response of the system. The model fits well the experimental results. The longest demonstrated delay of 7.5 ns was measured

using rubidium vapour at 141 °C. This value is only limited by the repetition rate of the excitation laser (~ 12.5 ns), and can reach much higher values, as shown in Fig. 3b. Note that at any time there is no more than one photon in the vapour cell, so the stream of photons after the cell will contain only single photons. We were thus able to store single photons in the rubidium cell for ~ 15 times their temporal width (500 ps; ref. 9). This demonstrates non-classical light storage of single photons generated on demand. Moreover, this scheme has small losses and dispersion and large bandwidth.

We also measured the degree of circular polarization of photons emitted from the Zeeman-split quantum dot exciton¹⁸ and slowed down in the vapour cell (see Supplementary Information). The data show that the polarization of photons is preserved during propagation through the cell. This result demonstrates that our rubidium vapour cell delay line can be used as a quantum memory in which a quantum state encoded in the polarization degrees of freedom of photons¹⁹ can be controllably stored.

We emphasize, here, that in spite of spectral diffusion in our quantum dots, the conclusions of the experiment will remain the same for quantum dots that do not suffer from charge fluctuations in their vicinity. For a spectrally isolated quantum dot, nearly 100% of emitted photons propagating through an atomic cell can be slowed down, yielding an efficient quantum memory for the transmitted photons. Adding two additional lasers resonant with the D_2 transitions would saturate the atoms⁴, and the original single-photon pulse can be retrieved on demand. Furthermore, as has recently been demonstrated²⁰, microcells containing atomic vapour can be integrated in semiconductor devices, enabling scalable on-chip photonic memories. The coupling of single

quantum dot emission to atomic vapours can now open exciting new avenues where the scalability and functionality of nanostructure devices based on single quantum dots can be combined with the uniformity of atomic systems in hybrid interfaces.

Methods

Sample. The quantum dots were GaAs inclusions in an AlGaAs matrix and were fabricated by molecular beam epitaxy in a multistep self-assembly process²¹. A template of Stranski–Krastanow InAs/GaAs quantum dots was first created. The sample surface was then capped by GaAs, and the InAs dots were removed by *in situ* etching, leaving holes on the GaAs surface. After growing a 10-nm-thick Al_{0.35}Ga_{0.65}As layer, the sample surface still had nanoholes, which were filled with GaAs to form the quantum dots used here. Finally, an Al_{0.45}Ga_{0.55}As layer was grown. The thickness of the GaAs layer connecting the quantum dots was optimized to 4 nm so that the quantum dot photoluminescence was close to 780 nm (ref. 14). The density of the quantum dots in the sample was low so that an individual quantum dot could be addressed easily.

Vapour cell. We used isotopically pure ⁸⁷Rb in a 75-mm-long quartz cell with antireflection coating.

Experimental set-up. Micro-photoluminescence studies were performed at 4.2 K in a helium bath cryostat with a 9 T superconducting magnet. The quantum dot was excited with 532 nm continuous-wave or 745 nm picosecond pulsed lasers focused to a spot size of 1 μm using a microscope objective with a numerical aperture of 0.85. The photoluminescence signal was collected by the same objective and was sent through a vapour cell to a spectrometer, which dispersed the photoluminescence onto a Peltier-cooled silicon array detector or a single photon detector, enabling 30 μeV spectral and 500 ps temporal resolution, respectively. The vapour cell was located ~1.5 m away from the cryostat.

Model. Our model was based on the following considerations. A wave packet composed of many frequency components can travel at very different velocities, much faster or much slower, than the individual waves forming the packet. The refractive index of the media sets the group velocity v_g ,

$$v_g = \frac{c}{n + \omega(dn/d\omega)} \quad (1)$$

where n is the frequency-dependent refractive index of the material and ω is the angular frequency. As the group velocity is inversely proportional to the derivative $dn/d\omega$, a rapid change in n will significantly reduce v_g , resulting in slow light speeds and therefore delayed transmission through the media.

In our case, we tuned the emission of a quantum dot between the hyperfine structure of the D_2 transitions. The ground state of the D_2 transition consists of two Lorentzian absorption resonances. This double absorption resonance media can be described by the electrical susceptibility χ (ref. 4),

$$\chi = A \left(\frac{g_1}{\omega_1 - \omega - i\gamma} + \frac{g_2}{\omega_2 - \omega - i\gamma} \right) \quad (2)$$

where g_1 and g_2 are the transition strengths, ω_1 and ω_2 are the transition frequencies, 2γ is the homogeneous linewidth, and A is the total strength of the resonance, with $A \propto N$, where N is the rubidium vapour density, which increases exponentially with temperature. The refractive index n and the extinction coefficient k of the media are derived directly from the susceptibility χ :

$$n = \text{Re}\sqrt{1 + \chi}, \quad k = \text{Im}\sqrt{1 + \chi} \quad (3)$$

The temperature sets the density of rubidium atoms, which sets the refractive index of the media seen by photons during their propagation through the cell.

Based on equations (1) to (3), we developed a theoretical model that accurately demonstrates the time evolution of photons comprising the emission line of a quantum dot, while taking into account realistic experimental parameters such as a lifetime of 500 ps (ref. 14), inhomogeneous broadening of the quantum dot emission of 80 μeV due to charge fluctuations in the GaAs buffer layer in the vicinity of the quantum dot, Doppler broadening of the rubidium atoms, and a temporal resolution of the measurement system of 500 ps. In the calculations, a detection pulse is modelled as an exponential decay convoluted with the temporal response of the system. An inhomogeneously broadened photoluminescence spectrum is modelled as a Gaussian. First, we calculated a transmission and a delay for each frequency in the region of [−30, 30] GHz. We then shifted the detection pulse according to the calculated delay. At the last stage, for each frequency we took a product of the shifted detection pulse, the photoluminescence spectrum and the

transmission. The result is the time-resolved frequency spectrum of the transmitted photoluminescence. Atomic density is the only free parameter in the model.

Received 17 October 2010; accepted 13 January 2011;
published online 20 February 2011

References

1. Michler, P. *et al.* A quantum dot single-photon turnstile device. *Science* **290**, 2282–2285 (2000).
2. Akopian, N. *et al.* Entangled photon pairs from semiconductor quantum dots. *Phys. Rev. Lett.* **96**, 130501 (2006).
3. Hau, L. V., Harris, S. E., Dutton, Z. & Behroozi, C. H. Light speed reduction to 17 metres per second in an ultracold atomic gas. *Nature* **397**, 594–598 (1999).
4. Camacho, R. M., Pack, M. V., Howell, J. C., Schweinsberg, A. & Boyd, R. W. Wide-bandwidth, tunable, multiple-pulse-width optical delays using slow light in cesium vapor. *Phys. Rev. Lett.* **98**, 153601 (2007).
5. Liu, C., Dutton, Z., Behroozi, C. H. & Hau, L. V. Observation of coherent optical information storage in an atomic medium using halted light pulses. *Nature* **409**, 490–493 (2001).
6. Phillips, D. F., Fleischhauer, A., Mair, A., Walsworth, R. L. & Lukin, M. D. Storage of light in atomic vapor. *Phys. Rev. Lett.* **86**, 783–786 (2001).
7. Briegel, H.-J., Dür, W., Cirac, J. I. & Zoller, P. Quantum repeaters: the role of imperfect local operations in quantum communication. *Phys. Rev. Lett.* **81**, 5932–5935 (1998).
8. Boller, K.-J., Imamolu, A. & Harris, S. E. Observation of electromagnetically induced transparency. *Phys. Rev. Lett.* **66**, 2593–2596 (1991).
9. Chanelière, T. *et al.* Storage and retrieval of single photons transmitted between remote quantum memories. *Nature* **438**, 833–836 (2005).
10. Eisaman, M. D. *et al.* Electromagnetically induced transparency with tunable single-photon pulses. *Nature* **438**, 837–841 (2005).
11. Bajcsy, M. *et al.* Efficient all-optical switching using slow light within a hollow fiber. *Phys. Rev. Lett.* **102**, 203902 (2009).
12. Slepkov, A. D., Bhagwat, A. R., Venkataraman, V., Londero, P. & Gaeta, A. L. Spectroscopy of Rb atoms in hollow-core fibers. *Phys. Rev. A* **81**, 053825 (2010).
13. Wu, B. *et al.* Slow light on a chip via atomic quantum state control. *Nature Photon.* **4**, 776–779 (2010).
14. Akopian, N. *et al.* Tuning single GaAs quantum dots in resonance with a rubidium vapor. *Appl. Phys. Lett.* **97**, 082103 (2010).
15. Ashoori, R. C. Electrons in artificial atoms. *Nature* **379**, 413–419 (1996).
16. Poem, E. *et al.* Polarization sensitive spectroscopy of charged quantum dots. *Phys. Rev. B* **76**, 235304 (2007).
17. Harris, S. E., Field, J. E. & Kasapi, A. Dispersive properties of electromagnetically induced transparency. *Phys. Rev. A* **46**, R29–R32 (1992).
18. Bayer, M. *et al.* Fine structure of neutral and charged excitons in self-assembled In(Ga)As/(Al)GaAs quantum dots. *Phys. Rev. B* **65**, 195315 (2002).
19. Bouwmeester, D. *et al.* Experimental quantum teleportation. *Nature* **390**, 575–579 (1997).
20. Kübler, H., Shaffer, J. P., Baluktian, T., Löw, R. & Pfau, T. Coherent excitation of Rydberg atoms in micrometre-sized atomic vapour cells. *Nature Photon.* **4**, 112–116 (2010).
21. Rastelli, A. *et al.* Hierarchical self-assembly of GaAs/AlGaAs quantum dots. *Phys. Rev. Lett.* **92**, 166104 (2004).

Acknowledgements

The authors acknowledge U. Perinetti, M. Koole and J. van Leeuwen for their help in the early stages of the project. The authors also thank L. Kouwenhoven for support and useful discussions. O. Benson and D. Hoeckel are acknowledged for their help with the vapour cell temperature control, and E. Zallo, R. Trotta, P. Atkinson and C. Deneke for their contributions to sample preparation. This work was supported by the Dutch Organization for Fundamental Research on Matter (FOM), The Netherlands Organization for Scientific Research (NWO Veni/Vidi), the German Research Foundation (DFG FOR 730) and the Federal Ministry of Education and Research (BMBF QK_QuaHL-Rep, 01BQ1032).

Author contributions

The experiments were conceived and designed by N.A. and V.Z. and carried out by N.A. The data were analysed and modelled by N.A. The sample was developed by L.W., A.R. and O.G.S. The manuscript was written by N.A. and V.Z. with input from A.R. and O.G.S.

Additional information

The authors declare no competing financial interests. Supplementary information accompanies this paper at www.nature.com/naturephotonics. Reprints and permission information is available online at <http://npg.nature.com/reprintsandpermissions/>. Correspondence and requests for materials should be addressed to N.A.